AD-A140 688 TRANSMISSION SYSTEM DEVELOPMENT FOR ELECTRON CYCLOTRON 1/0
HEATING EXPERIMENTS OF A TOKAMAK PLASMA(U) JAYCOR
ALEXANDRIA VA J S LEVINE 02 APR 84
UNCLASSIFIED JAYCOR-J206-84-007/6213 N00014-81-C-2218 F/G 9/5 NL

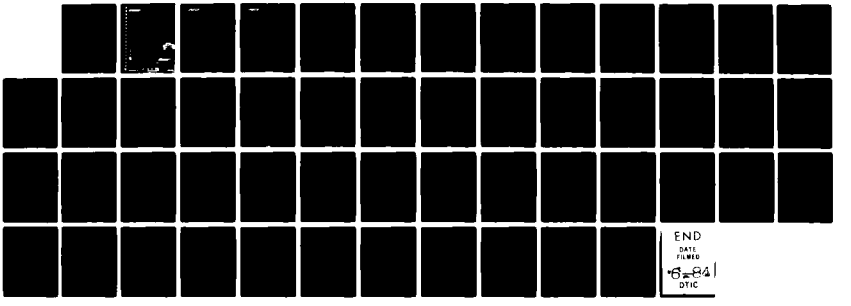

END
DATE FILMED
6-84
DTIC

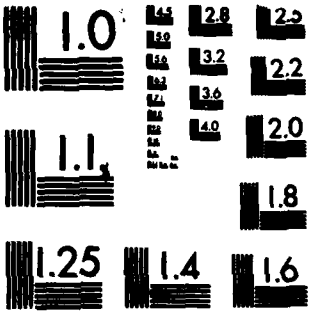

JAYCOR

6213

April 2, 1984

Dr. Michael Read
Code 4740
Naval Research Laboratory
4555 Overlook Avenue, SW
Washington, DC 20375

SUBJECT: Final, Design and Test Report, Contract Number N00014-81-C-2218

Dear Dr. Read:

JAYCOR is pleased to submit these Final, Design and Test Reports entitled, *Transmission System Development for Electron Cyclotron Heating Experiments of a Tokamak Plasma*, in accordance with the subject contract, CDRL Item Numbers A002, A003 and A004.

If these reports are acceptable, please sign and forward the enclosed DD Form 250.

Questions of a technical nature should be addressed to Mr. Roger Behrendt while questions of a contractual nature should be addressed to Mr. Floyd C. Stilley, our Contracts Administrator.

Sincerely,

Martin C. Nielsen
Vice President
and Counsel

ssh-b

Enclosures

cc: Code 1232.BB
Code 2627
DTIC

JAYCOR

TRANSMISSION SYSTEM DEVELOPMENT FOR ELECTRON CYCLOTRON HEATING EXPERIMENTS OF A TOKAMAK PLASMA

J206-84-007/6213

Final, Design and Test Reports

by

Jerrold S. Levine*

April 2, 1984

Prepared for

Naval Research Laboratory
4555 Overlook Avenue, SW
Washington, DC 20375

Under:

Contract Number N00014-81-C-2218

*Present address: Naval Research Laboratory
Washington, DC 20375

UNCLASSIFIED

SECURITY CLASSIFICATION OF THIS PAGE (When Data Entered)

REPORT DOCUMENTATION PAGE		READ INSTRUCTIONS BEFORE COMPLETING FORM
1. REPORT NUMBER J206-84-007/6213	2. GOVT ACCESSION NO.	3. RECIPIENT'S CATALOG NUMBER
4. TITLE (and Subtitle) Transmission System Development for Electron Cyclotron Heating Experiments of a Tokamak Plasma		5. TYPE OF REPORT & PERIOD COVERED Final Report: 05/13/81 thru 07/12/82 6. PERFORMING ORG. REPORT NUMBER J206-84-007/6213
7. AUTHOR(s) Jerrold S. Levine		8. CONTRACT OR GRANT NUMBER(s) N00014-81-C-2218
9. PERFORMING ORGANIZATION NAME AND ADDRESS JAYCOR 205 South Whiting Street Alexandria, VA 22304		10. PROGRAM ELEMENT, PROJECT, TASK AREA & WORK UNIT NUMBERS A002, A003 and A004
11. CONTROLLING OFFICE NAME AND ADDRESS Naval Research Laboratory 4555 Overlook Avenue, SW Washington, DC 20375		12. REPORT DATE April 2, 1984 13. NUMBER OF PAGES 43 pages
14. MONITORING AGENCY NAME & ADDRESS(if different from Controlling Office)		15. SECURITY CLASS. (of this report) UNCLASSIFIED 15a. DECLASSIFICATION/DOWNGRADING SCHEDULE

16. DISTRIBUTION STATEMENT (of this Report)

1 copy - Code 4740
1 copy - Code 1232.BB
6 copies - Code 2627
12 copies - DTIC

This document has been approved for public release and sale; its distribution is unlimited

17. DISTRIBUTION STATEMENT (of the abstract entered in Block 20, if different from Report)

18. SUPPLEMENTARY NOTES

19. KEY WORDS (Continue on reverse side if necessary and identify by block number)

20. ABSTRACT (Continue on reverse side if necessary and identify by block number)

We present the general theory of rippled wall mode converters. Coupling coefficients for TE and TM waves, of both fixed and rotating polarizations, are calculated. The waveguide ripples considered may be axisymmetric, fluted or helical. We describe in detail a 97 percent TE_{04}/TE_{01} converter designed for use with a 35 GHz gyrotron. Cold test results confirm its performance. We also present a compilation of engineering drawings developed for the construction of the antenna or transmission system.

DD FORM 1 JAN 73 1473 EDITION OF 1 NOV 65 IS OBSOLETE
S/N 0102-LF-014-6601

UNCLASSIFIED
SECURITY CLASSIFICATION OF THIS PAGE (When Data Entered)

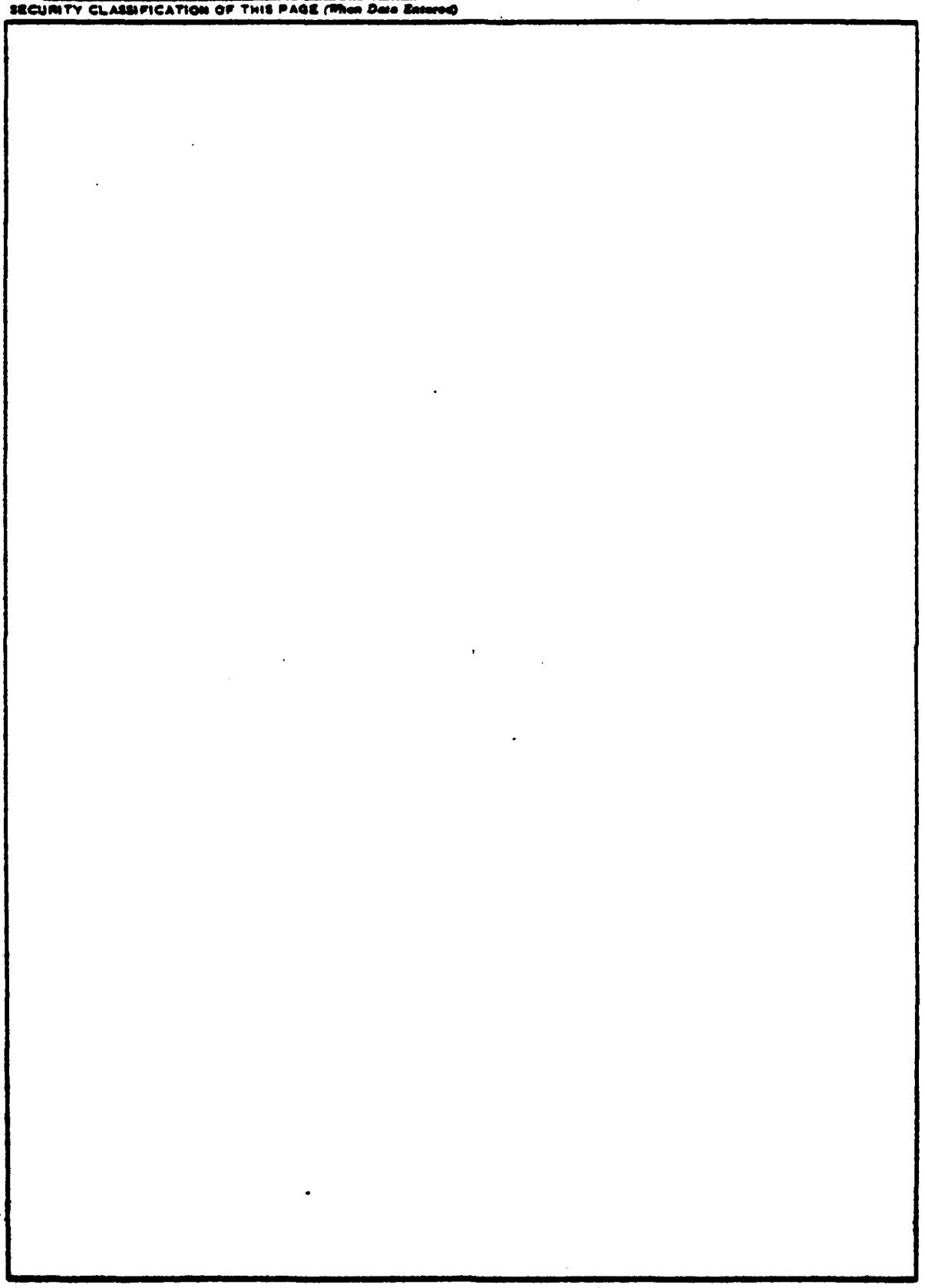

TABLE OF CONTENTS

5/11

@@ @@ A140888 (U) FIELD/GROUP @@@@@@

UNCLASSIFIED TITLE

TRANSMISSION SYSTEM DEVELOPMENT FOR ELECTRON CYCLOTRON HEATING EXPERIMENTS OF A TOKAMAK PLASMA.

ABSTRACT

(U) THE HEATING OF TOKAMAK PLASMAS BY MICROWAVES AT ELECTRON CYCLOTRON FREQUENCY HAS BEEN THE SUBJECT OF INVESTIGATION FOR SEVERAL YEARS BY SEVERAL GROUPS INCLUDING THE NAVAL RESEARCH LABORATORY (NRL). TO ENABLE ELECTRON CYCLOTRON HEATING (ECH) TO PRODUCE SIGNIFICANT TEMPERATURE INCREASES, THE INCIDENT MICROWAVE POWER MUST BE AS STRONG AS, OR STRONGER THAN, THE OHMIC HEATING POWER REQUIRED FOR THE TOKAMAK DISCHARGE. HOWEVER, ECH EXPERIMENTS ARE LIMITED TO THE CURRENT AVAILABLE MICROWAVE POWER. TO ADDRESS THE ISSUE OF MICROWAVE POWER, NRL DESIGNED, BUILT AND TESTED A HIGH POWER (APPROX. 300 KW) GYROTRON FOR OPERATION AT A 1 MICROSEC PULSE LENGTH. IN ORDER TO USE THIS SOURCE FOR ECH EXPERIMENTS, A TRANSMISSION SYSTEM WAS DESIGNED AND BUILT THAT POLARIZED THE MICROWAVES FOR OPTIMAL HEATING EFFICIENCY AND COUPLED THEM INTO THE TOKAMAK PLASMA WITH MINIMAL LOSS. THE DEVELOPMENT OF THE TRANSMISSION SYSTEM IS THE TOPIC OF THIS FINAL REPORT. THE REPORT CONSISTS OF TWO PARTS. FIRST IS A PAPER DESCRIBING THE SUBJECT OF RIPPLED WALL MODE CONVERTERS FOR CIRCULAR WAVEGUIDES. THE SECOND PART IS A COMPILATION OF THE ENGINEERING DRAWINGS DEVELOPED FOR THE CONSTRUCTION OF THE ANTENNA OR TRANSMISSION SYSTEM.

POSTING TERMS ASSIGNED

CIRCULAR WAVEGUIDES
USE CIRCULAR
WAVEGUIDES

CONSTRUCTION OF THE ANTENNA
USE ANTENNAS
CONSTRUCTION

ELECTRON CYCLOTRON HEATING
USE CYCLOTRONS
HEATING

ELECTRON CYCLOTRON HEATING EXPERIMENTS
USE CYCLOTRONS
HEATING

ENGINEERING DRAWINGS
USE ENGINEERING DRAWINGS

HIGH POWER
USE HIGH POWER

MICROWAVE POWER
USE MICROWAVES
RADIOFREQUENCY POWER

MICROWAVES
USE MICROWAVES

NAVAL RESEARCH LABORATORY
USE NAVAL RESEARCH LABORATORIES

OPTIMAL HEATING EFFICIENCY
USE EFFICIENCY
HEATING
OPTIMIZATION

PULSE LENGTH
USE LENGTH
PULSES

TOKAMAK PLASMA
USE PLASMAS(PHYSICS)
TOKAMAKS

TOKAMAK PLASMAS

TRANSMISSION SYSTEM

UNCLASSIFIED

USE PLASMAS(PHYSICS)
TOKAMAKS

TRANSMISSION SYSTEM DEVELOPMENT
USE TRANSMITTANCE

USE TRANSMITTANCE

WALL MODE CONVERTERS
USE CONVERTERS
WALLS

PHRASES NOT FOUND DURING LEXICAL DICTIONARY MATCH PROCESS

300 KW

I. INTRODUCTION

The heating of tokamak plasmas by microwaves at electron cyclotron frequency has been the subject of investigation for several years by several groups including the Naval Research Laboratory (NRL). To enable electron cyclotron heating (ECH) to produce significant temperature increases, the incident microwave power must be as strong as, or stronger than, the ohmic heating power required for the tokamak discharge. However, ECH experiments are limited to the current available microwave power.

To address the issue of microwave power, NRL designed, built and tested a high power (~300 kW) gyrotron for operation at a 1 microsec pulse length. In order to use this source for ECH experiments, a transmission system was designed and built that polarized the microwaves for optimal heating efficiency and coupled them into the tokamak plasma with minimal loss.

The development of the transmission system is the topic of this Final Report. The report consists of two parts. First is a paper describing the subject of rippled wall mode converters for circular waveguides. The second part is a compilation of the engineering drawings developed for the construction of the antenna or transmission system.

II. RIPPLED WALL MODE CONVERTERS FOR CIRCULAR WAVEGUIDES

ABSTRACT

We present the general theory of rippled wall mode converters. Coupling coefficients for TE and TM waves, of both fixed and rotating polarizations, are calculated. The waveguide ripples considered may be axisymmetric, fluted or helical. We describe in detail a 97 percent TE_{04}/TE_{01} converter designed for use with a 35 GHz gyrotron. Cold test results confirm its performance.

INTRODUCTION

Gyrotron oscillators are efficient sources of high power, mm wavelength radiation. Their output, however, is often in a high order TE_{nm} circular waveguide mode that is not convenient to use in a variety of applications[1]. Thus, it is desirable to transform the gyrotron output to a lower order mode, ideally TE_{01} or TE_{11}. Due to the high powers and frequencies involved, the process must, in general, take place in overmoded waveguide.

One approach to mode conversion relies on the fact that an arbitrary perturbation to an otherwise uniform waveguide causes coupling between all waveguide modes[2]. By using a prescribed perturbation, with proper axial and azimuthal symmetry, efficient mode conversion can be realized[3,4]. The perturbation is a ripple at the beat wavelength between the input (gyrotron) mode and the desired output mode (see Figure 1). An axisymmetric structure

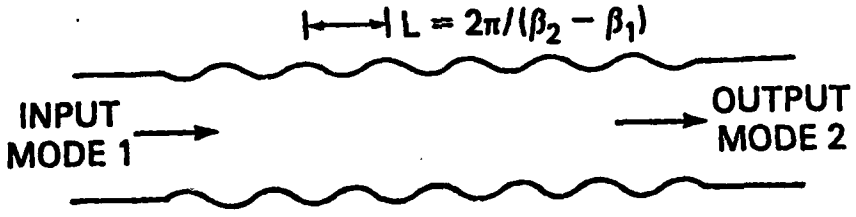

Figure 1 The rippled wall mode converter transforms one mode to another by a periodic perturbation at the beat wavelength of the two modes.

preserves the azimuthal mode number while a fluted or helical structure can change both radial and azimuthal mode numbers. The ripple couples all the modes, subject to azimuthal selectivity rules, but coherent energy transfer occurs only between the design modes. The incoherence of the coupling between other modes provides for little net energy transfer in a mode converter that is several ripple periods long.

In this paper we present the general theory of rippled wall mode converters. As in Reference 4, we employ the coupled wave equation[5], but do not make the assumption that all modes are far from cutoff. We further extend previous work[3,4] to include both TE and TM waves and treat non-axisymmetric equations that yield some insight and scaling laws that are useful for a first order design. Finally, we describe a TE_{04}/TE_{01} converter for use with a $\gtrsim$ 300 kW, 35 GHz gyrotron[6,7]. Cold test data is presented and compared with calculated performance.

COUPLED WAVE EQUATIONS

Propagation in a slightly irregular waveguide can be described by a set of coupled wave equations[5] for the (complex) amplitude, A_j, of each mode (with temporal dependence $e^{i\omega t}$)

$$\frac{dA_j}{dz} = -i\beta_j A_j + \sum_{k\neq j} K_{jk}A_k. \qquad [1]$$

The coupling coefficients between modes, K_{jk}, depend both on the type of perturbation and the type of modes involved[2]. The wavenumber, β, is taken as appropriate for a

uniform waveguide of the local average radius. We consider only forward-going, propagating waves. Coupling to a backward-going wave would be significant only for a mode going through cutoff or for an abrupt change in cross section.

There are two forms of perturbation with which we are concerned here: non-rotating (NR) and rotating (R) variations of the radius (flutes and helices, respectively)

$$a(z) = \begin{cases} a_0 + a_1 \sin(kz)\cos(q\phi) & (NR) \\ a_0 + a_1 \sin(kz - q\phi) & (R) \end{cases} \qquad [2]$$

The non-rotating ripples will be useful for conversion between non-rotating modes [$\cos(n\phi)$ (A^c) or $\sin(n\phi)$ (A^s) azimuthal dependence]; the rotating ripples will be useful for right-hand and left-hand polarized rotating modes [$A^{\pm} = (A^c \pm iA^s)/\sqrt{\varepsilon}$; $\varepsilon = 1$ for axisymmetric modes, $\varepsilon = 2$ otherwise].

For non-rotating modes in waveguide with non-rotating perturbations (NR/NR), the mode types decouple in pairs; TE^c/TM^s and TE^s/TM^c. No such decoupling occurs between rotating modes in waveguide with rotating perturbations (R/R). Writing H for the amplitudes of TE modes and E for the amplitudes of TM modes, the coupled wave equations are:

<u>NR/NR</u>; <u>TE^c/TM^s</u>

$$\frac{dH_j}{dz} = -i\beta_j H_j + \sum_k \left\{ S_{jk}^{TE/TE} H_k \,(D1 + D2 + D3 + D4) + S_{jk}^{TE/TM} E_k \,(D1 + D4 - D2 - D3) \right\} \cos(kz) \qquad [3]$$

$$\frac{dE_j}{dz} = -i\beta_j E_j + \sum_k \left\{ S_{jk}^{TM/TM} E_k (D2 + D3 - D1 - D4) + S_{jk}^{TM/TE} H_k (D1 + D4 - D2 - D3) \right\} \cos(kz)$$

NR/NR; TE^s/TM^c

$$\frac{dH_j}{dz} = -i\beta_j H_j + \sum_k \left\{ S_{jk}^{TE/TE} H_k (D2 + D3 - D1 - D4) + S_{jk}^{TE/TM} E_k (D1 + D2 + D3 + D4) \right\} \cos(kz) \qquad [4]$$

$$\frac{dE_j}{dz} = -i\beta_j E_j + \sum_k \left\{ S_{jk}^{TM/TM} E_k (D1 + D2 + D3 + D4) + S_{jk}^{TM/TE} H_k (D1 + D2 + D3 + D4) \right\} \cos(kz)$$

R/R

$$\frac{dH_j^{\pm}}{dz} = -i\beta_j H_j^{\pm} + \sum_k \sqrt{\frac{\varepsilon_g}{\varepsilon_n}} \left\{ S_{jk}^{TE/TE} \left[H_k^{\pm}(D2e^{\pm ikz} + D3e^{\mp ikz}) + H_k^{\mp}(D4e^{\pm ikz} + D1e^{\mp ikz}) \right] \pm iS_{jk}^{TE/TM} \left[E_k^{\pm}(D3e^{\pm ikz} + D2e^{\mp ikz}) + E_k^{\mp}(D4e^{\pm ikz} + D1e^{\mp ikz}) \right] \right\} \qquad [5]$$

$$\frac{dE_j^{\pm}}{dz} = -i\beta_j E_j^{\pm} + \sum_k \sqrt{\frac{\varepsilon_g}{\varepsilon_n}} \left\{ S_{jk}^{TM/TM} \left[E_k^{\pm}(D2e^{\pm ikz} + D3e^{\mp ikz}) + \right. \right.$$

$$E_k^{\mp}(D4e^{\pm ikz} + D1e^{\mp ikz})] \mp iS_{jk}^{TM/TE}[H_k^{\pm}(D2e^{\pm ikz} +$$

$$D3e^{\mp ikz}) - H_k^{\mp}(D4e^{\pm ikz} + D1e^{\mp ikz})]\}$$

where

$$S_{jk}^{TE/TE} = \frac{\sqrt{\epsilon_g \epsilon_n}}{2} \frac{1}{x_{gh}^2 - x_{nm}^2} \left\{ x_{gh}^2 \left[\frac{(x_{nm}^2 - n^2) Z_{gh}}{(x_{gh}^2 - g^2) Z_{nm}} \right]^{1/2} + \right.$$

$$\left. x_{nm}^2 \left[\frac{(x_{gh}^2 - g^2) Z_{nm}}{(x_{nm}^2 - n^2) Z_{gh}} \right]^{1/2} \right\} \frac{ka_1}{a_0}$$

$$S_{jk}^{TE/TM} = \frac{n\sqrt{\epsilon_g \epsilon_n}}{2} \left[\frac{Z_{nm}}{(x_{nm}^2 - n^2) Z_{gh}} \right]^{1/2} \frac{ka_1}{a_0} \qquad [6]$$

$$S_{jk}^{TM/TM} = \frac{\sqrt{\epsilon_g \epsilon_n}}{2} \frac{1}{w_{gh}^2 - w_{nm}^2} \left[w_{nm}^2 \left(\frac{Z_{gh}}{Z_{nm}} \right)^{1/2} + \right.$$

$$\left. w_{gh}^2 \left(\frac{Z_{nm}}{Z_{gh}} \right)^{1/2} \right] \frac{ka_1}{a_0}$$

$$S_{jk}^{TM/TE} = -\frac{g\sqrt{\epsilon_g \epsilon_n}}{2} \left[\frac{Z_{gh}}{(x_{gh}^2 - g^2) Z_{nm}} \right]^{1/2} \frac{ka_1}{a_0}$$

$$S_{jj}^{TE/TE} = S_{jj}^{TM/TM} = 0$$

$$\epsilon_p = \begin{cases} 1 & p = 0 \\ 2 & p > 0. \end{cases}$$

In equations [3] - [6],

$$D1 = \delta (q + n + g)$$
$$D2 = \delta (q + n - g)$$
$$D3 = \delta (q - n + g)$$
$$D4 = \delta (q - n - g), \qquad [7]$$

which provide azimuthal selectivity. The modes, their appropriate zeroes and wave impedances, are:

$$H_j = TE_{nm}; \quad J_n'(x_{nm}) = 0; \quad Z_{nm} = Z_0\beta_0/\beta_{nm}$$

$$H_k = TE_{gh}; \quad J_g'(x_{gh}) = 0; \quad Z_{gh} = Z_0\beta_0/\beta_{gh}$$

$$E_j = TM_{nm}; \quad J_n(w_{nm}) = 0; \quad Z_{nm} = Z_0\beta_{nm}/\beta_0 \qquad [8]$$

$$E_k = TM_{gh}; \quad J_g(w_{gh}) = 0; \quad Z_{gh} = Z_0\beta_{gh}/\beta_0$$

where β_0 and Z_0 are the wavenumber and impedance for free space propagation, respectively.

Axisymmetric modes can be considered as either rotating or non-rotating modes. The TE_{0m} (TM_{0m}) modes are H^c (E^c) only, when considered NR/NR, but must be included as both H^+ and H^- (E^+ and E^-) in the R/R summations.

From Equation [6], we observe that modes near cutoff couple strongly to all other modes as their impedance approaches infinity (zero) for TE (TM) modes. Tight coupling of neighboring modes is indicated by the "resonance" denominators in $S_{jk}^{TE/TE}$ and $S_{jk}^{TM/TM}$. We further note

that TE_{0m} modes do not couple to TM modes and, from Equation [7], that axisymmetric ripples (q = 0) do not couple modes with differing azimuthal mode numbers.

Complete characterization of a mode converter requires numerical integration of the coupled wave equations for each propagating mode. However, some insight and basic scaling laws can be obtained by considering only the two modes of interest, but allowing a mismatch between the beat period of the waves and the period of the ripple ($k = \beta_2 - \beta_1 + \delta$).

The coupled wave equations are:

$$\frac{dA_1}{dz} = -i\beta_1 A_1 + C \cos\left[(\beta_2 - \beta_1 + \delta)z\right]A_2$$

$$\frac{dA_2}{dz} = -i\beta_2 A_2 - C^* \cos\left[(\beta_2 - \beta_1 + \delta)z\right]A_1 \qquad [9]$$

where C can be evaluated in terms of S_{jk} for the proper wave and perturbation types. Appropriate manipulation and averaging over a scale length of half the ripple period yields

$$A_1 A_1^*(z) = \frac{1}{2(CC^* + \delta^2)}\left[CC^*\{1+\cos[(CC^*+\delta^2)^{1/2}z]\}+2\delta^2\right] \qquad [10]$$

$$A_2 A_2^*(z) = \frac{CC^*}{2(CC^* + \delta^2)}\{1 - \cos[(CC^* + \delta^2)^{1/2}z]\},$$

where all the energy is assumed to be in mode 1 at z = 0. When there is no mismatch ($\delta = 0$), all the energy is transferred to mode 2 at $z_c = \pi/C$, the length of the ideal converter. Defining the actual efficiency, η, as $A_2 A_2^*(z_c)$,

the bandwidth and criticality of dimension can be approximated by evaluating, at the design values,

$$\frac{dn}{dX} = 0; \quad \frac{d^2\eta}{dX^2} = -\frac{2z_c^2}{\pi^2}\left(\frac{d\delta}{dX}\right)^2 - \frac{z_c^2}{2}\left|\frac{dC}{dX}\right|^2 \qquad [11]$$

where X is any parameter of interest (e.g., f, a_0, a_1, $L = 2\pi/k$).

For conversion between TE_{nm} modes by axisymmetric ripples, straight forward evaluation yields:

$$z_c = \frac{\pi a_0}{a_1}\,\frac{x_2^2 - x_1^2}{\beta_2 - \beta_1}\left\{x_2^2\left[\frac{(x_1^2 - n^2)\,\beta_1}{(x_2^2 - n^2)\,\beta_2}\right]^{1/2} + x_1^2\left[\frac{(x_2^2 - n^2)\beta_2}{(x_1^2 - n^2)\beta_1}\right]^{1/2}\right\}^{-1}$$

$$\frac{d\delta}{df} = -\frac{f(\beta_2 - \beta_1)}{[(f^2 - f_{c1}^2)(f^2 - f_{c2}^2)]^{1/2}}$$

$$\frac{d\delta}{da_0} = -\frac{2\pi}{a_0 c}\left[\frac{f_{c1}^2}{(f^2 - f_{c1}^2)}^{1/2} - \frac{f_{c2}^2}{(f^2 - f_{c2}^2)}^{1/2}\right] \qquad [12]$$

$$\frac{d\delta}{dL} = \frac{2\pi}{L^2}$$

$$\frac{dC}{df} = \frac{4\pi^3}{c}\,\frac{fa_1}{La_0^3}\,\frac{1}{(\beta_1\beta_2)^{3/2}}\left\{\frac{x_1^2}{\beta_1}\left[\frac{x_2^2 - n^2}{x_1^2 - n^2}\right]^{1/2} -\right.$$

$$\frac{x_2^2}{\beta_2}\left[\frac{x_1^2 - n^2}{x_2^2 - n^2}\right]^{1/2}\Bigg\}$$

$$\frac{dC}{da_0} = \frac{4\pi^3}{c^2}\,\frac{f^2 a_1}{L a_0^4}\,\frac{1}{(\beta_1\beta_2)^{3/2}}\left\{\frac{x_1^2}{\beta_1}\left[\frac{x_2^2 - n^2}{x_1^2 - n^2}\right]^{1/2} - \frac{x_2^2}{\beta_2}\left[\frac{x_1^2 - n^2}{x_2^2 - n^2}\right]^{1/2}\right\} - \frac{\pi}{a_0 z_c}$$

$$\frac{dC}{da_1} = \frac{\pi}{a_1 z_c}$$

$$\frac{dC}{dL} = \frac{\pi}{L z_c}$$

where $f_c = cx/2\pi a_0$ is the cutoff frequency for the unperturbed waveguide. For $n = 0$, the converter length is

$$z_c = \frac{\pi a_0^3}{a_1}\,\frac{\sqrt{\beta_1\beta_2}}{x_1 x_2} \qquad [13]$$

which is the proper scaling law for all $x^2 >> n^2$.

From a more exact two mode analysis, that takes account of the nonlinear dependence of wavenumber on waveguide radius, we find that the optimal ripple period is slightly shorter than the beat period of the two modes in the unperturbed waveguide, L_0 [$= 2\pi/(\beta_2 - \beta_1)$],

$$L = L_0 \left[1 + \frac{a_1^2}{4a_0^4 (\beta_2 - \beta_1)} \left\{ 3 \left(\frac{\alpha_2^2}{\beta_2} - \frac{\alpha_1^2}{\beta_1}\right) + \frac{1}{a_0^2} \left(\frac{\alpha_2^4}{\beta_2^3} - \frac{\alpha_1^4}{\beta_1^3}\right)\right\}\right] \quad [14]$$

where α = x or w for TE or TM waves, respectively. However, when more than two modes are interacting, the nonresonant energy exchange with the other modes can modify the phases of the two modes of interest sufficiently to dominate this correction. L should thus be varied both above and below L_0 to optimize the conversion efficiency.

TE_{04}/TE_{01} MODE CONVERTER

The gyrotron we wish to use is a $\gtrsim$300 kW, TE_{04} source which operates at 35.95 GHz[6,7]. The output radius is 2.54 cm, which is cutoff to the Te_{06} mode and above. The presence of the TE_{05} mode interferes with conversion of the TE_{04} to TE_{01} because, as mentioned in the preceding section, being both near cutoff and adjacent to the TE_{04}, it interacts strongly. The converter is therefore designed with a_0 = 2.1 cm, with 2° tapers at either end. (Mode conversion in tapers can be analyzed in a fashion analogous to the above.) The chosen ripple amplitude is a_1 = 0.05 cm which requires 32 ripple periods.

As an illustration of the last point in the preceding section, we note that for this design, L_0 = 1.827 cm, and, according to Equation [14], the optimized L = 1.822 cm.

If only the TE_{01} and TE_{04} modes are included in the numerical integration, the two rippled periods included, the efficiencies drop to 95.9 percent and 89.1 percent. The peak conversion efficiency is 98.7 percent at L = 1.832 cm.

The characteristics of the conversion section are summarized in Table 1. Including the tapers, the converter is 80 cm long and 96.9 percent efficient. Figure 2 shows the calculated normalized power in each mode as a function of z. Power is conserved to 1 part in 10^5 in the calculation.

TABLE 1. MODE CONVERTER DESIGN CHARACTERISTICS

INPUT MODE	OUTPUT MODE	f (GHz)	a_0 (cm)	a_1 (cm)	L (cm)	z_c (cm)	η (%)	FWHM (GHz)
TE_{04}	TE_{01}	34.95	2.100	0.050	1.832	58.0	98.7	0.42
TE_{04}	TE_{01}	140.00	1.472	0.050	4.782	112.0	94.1	4.00
TE_{16}	TE_{12}	94.00	1.400	0.030	1.428	50.9	96.1	1.56
TE_{12}	TE_{11}	94.00	1.000	0.075	9.670	81.5	98.9	7.57

The frequency response, based on the two mode result, Equation [10], which allows 100 percent conversion, is shown in Figure 3 as the solid curve. The large number of ripples makes the converter a very narrow band device. A deviation of 60 MHz lowers the efficiency to 95 percent; the FWHM is only 420 MHz. Using Equations [11] and [12], the strictest machining tolerance is found to be on the unperturbed radius, a_0. A variation of 0.0024 cm from the

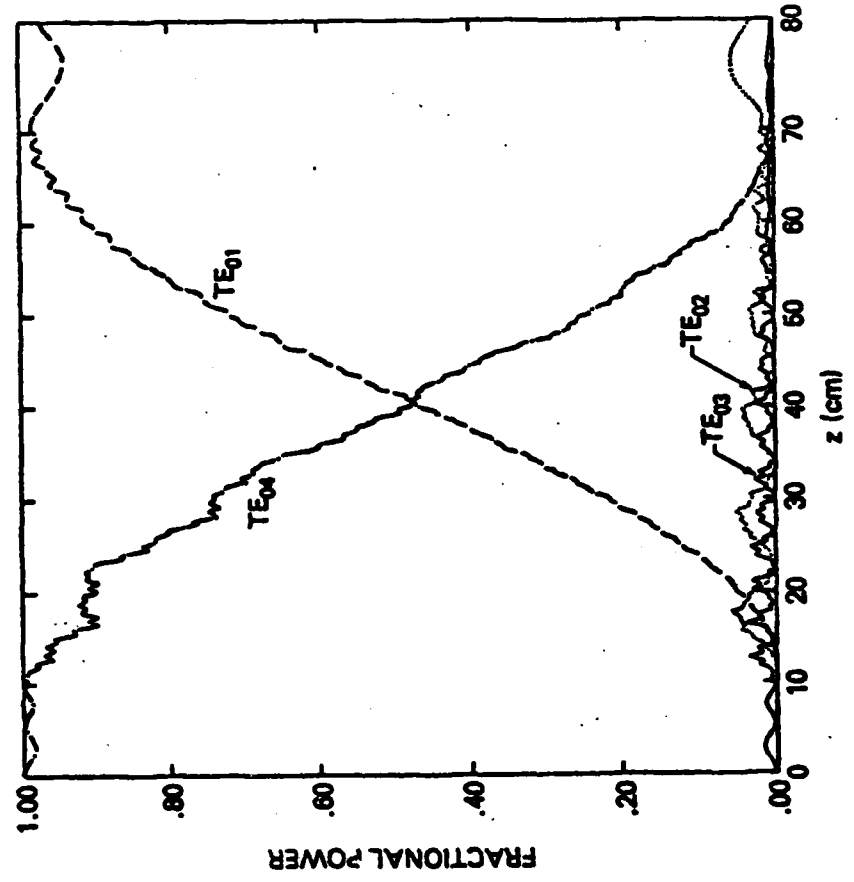

Figure 2 Calculated fractional power in each TE_{0m} mode for the mode converter described in the text. The input TE_{04} mode is converted to the TE_{01} mode with 98.9% efficiency.

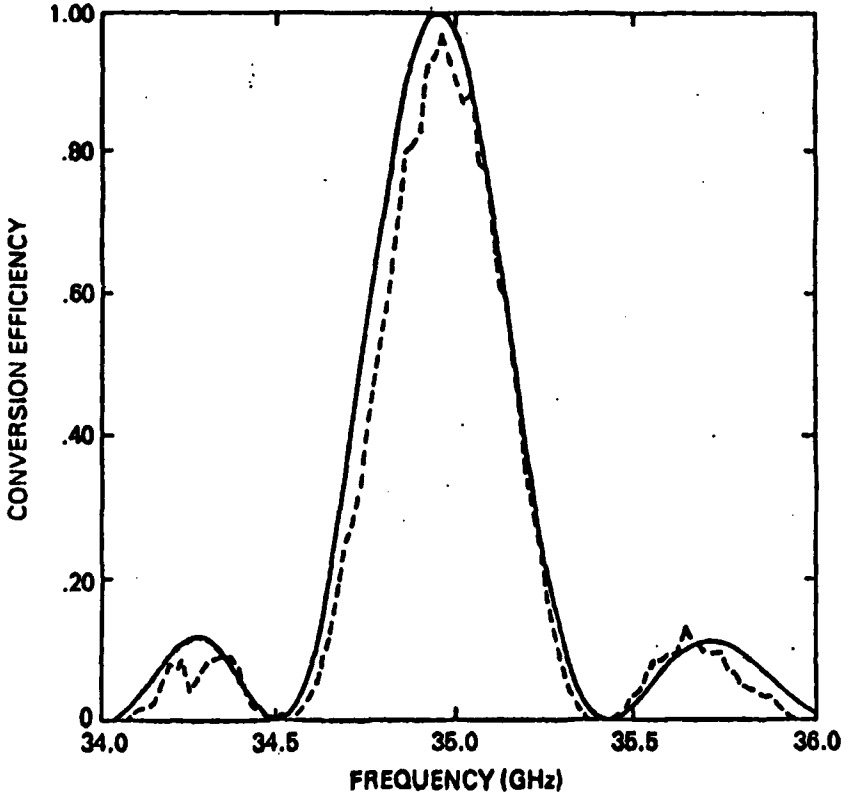

Figure 3 Calculated (solid curve) and measured (dashed curve) TE_{01}/TE_{04} conversion efficiency of the mode converter described in the text.

design value would limit the efficiency to 95 percent. (This is a tolerance of ±1.9 mil in the diameter, and is readily obtainable.) The peak electric field for 300 kW in the TE_{04} mode is 21.6 kV/cm, which does not present any particular breakdown problems.

A mode converter of the above dimensions was electroformed using a mandrell machined on a numerically controlled lathe. For cold test purposes, a TE_{01} mode was used as the input, and the conversion to TE_{04} measured. The various modes were distinguished by their far field radiation patterns. [There are angles, determined by the Bessel function roots, where each of the Te_{0m} modes can be individually identified[8].] The measured conversion efficiency is shown as the dashed curve in Figure 3. The agreement with the simple model, even to the side lobes, is excellent. The peak conversion efficiency is 96 ± 5 percent and occurs at the design frequency. This should be compared with the efficiency calculated for conversion from TE_{01} to TE_{04}, which is 97.4 percent at 34.95 GHz.

DISCUSSION

It is often advantageous to use a waveguide that is sufficiently large that both modes of interest are far from cutoff. A TE_{04}/TE_{01} converter for 140 GHz we designed illustrates the considerations (see Table 1). Making a_0 small enough to cutoff modes above the TE_{04} limits the power handling capability and demands very tight machining tolerances. Increasing a_0 slightly brings in higher order modes, near cutoff, that couple strongly to the TE_{04}; the mismatch between the beat period and the ripple periods is insufficient

to suppress their excitation. However, by increasing a_0 further, the modes near cutoff are far enough removed from the TE_{04} that no competing interaction "overwhelms" the desired conversion. A final design that features broad bandwidth, realistic machining tolerances, high power handling capability and 94 percent conversion efficiency was obtained for waveguide that propagates up to the $TE_{0,13}$ mode.

It is not always practical to transform directly between the modes of interest, as we have done above. As an example, consider a TE_{16}/TE_{11} converter at 94 GHz with a power handling capacity of 1 MW (see Table 1). By following the above prescription, we would have arrived at the design of a mode converter that was several meters long. Instead, by using the TE_{12} mode as an intermediate stage, we designed two mode converters, each of which feature all the desired characteristics, that together are less than 1.4 m long, including a taper section that joins them.

We have shown that the rippled wall mode converter is an efficient device for matching the constraints of high power, high frequency mm wave production on the one hand, and the constraints of transmission systems and final applications on the other hand. Based on the analysis presented here it is possible to design converters that change the azimuthal as well as radial mode numbers, the rotating or non-rotating characteristic of the wave, and even whether the mode is TE or TM.

ACKNOWLEDGMENTS

This work has benefited from discussions with Drs. M. Bollen, K.R. Chu, C. Moeller and M. Read. It was supported by the U.S. Department of Energy, Contract Numbers DE-AI01-77ET43029 and DE-AI01-80ER52065 through the Naval Research Laboratory, Contract Number N00014-81-C-2218.

REFERENCES

1. K.J. Kim, M.E. Read, J.M. Baird, K.R. Chu, A. Drobot, J.L. Vomvoridis, A. Ganguly, D. Dialetis and V.L. Granatstein, Int. J. Electron., 51, 427 (1981).

2. L. Solymar, IEEE Trans., MTT-7, 379 (1959).

3. N.F. Kovalev, I.M. Orlov and M.I. Peletin, Radio Phys. Quant. Electron., 11, 449 (1969).

4. C. Moeller, Int. J. Electron., 53, 587 (1982).

5. S.A. Schelkunoff, Bell Syst. Tech. J., 34, 995 (1955).

6. B. Arfin, K.R. Chu, D. Dialetis and M.E. Read, IEEE Trans., ED-29, 1911 (1982).

7. Y. Carmel, K.R. Chu, M. Read, A.K. Ganguly, D. Dialetis, R. Seeley, J.S. Levine and V.L. Granatstein, Phys. Rev. Lett., 50, 112 (1983).

8. J.R. Risser, Microwave Antenna Theory and Design (ed. S. Silver), pg. 334-337 (1949). McGraw Hill, New York.

III. ANTENNA DESIGN

A microwave antenna (transmission system) was designed and subsequently built at the Naval Research Laboratory. The figures presented in this section are the component design drawings with the assembly pictured in Figure 18. There has been no attempt to draw the items to scale. A brief discussion of each figure is given in the following paragraph.

The main flange is shown in Figure 1. It has a knife edge in the bottom to mate with the 4.5 inch conflat port flange on ISX. The two holes drilled in the side are for feeding the wire rope. The angles were calculated so that the wire rope feeds in tangentially and the holes miss the conflat bolt circle. Hole A in the diagram feeds the wire rope in/out at the bottom and is offset closer to the bottom of the flange. Similarly, hole B is the upper feed and is offset closer to the top of the flange. The notch for this hole is required for assembly.

The VESPEL bearing (Figure 2) sits in the bottom of the flange. It is half cut away for pumping. While this is free to spin, it is not intended to be rotating. The intended bearing surface is the upper surface upon which the metal ring (Figure 3) rotates. The thin tip on the ring points up and is welded to the waveguide, supporting its weight.

The wire rope that turns the antenna feeds onto the VESPEL spool shown in Figure 4. The rectangular notch in the side accepts the insert (Figure 5) which is welded to the wire rope at the hole (A). The interior notches in the spool rotate the antenna via tabs welded onto the antenna.

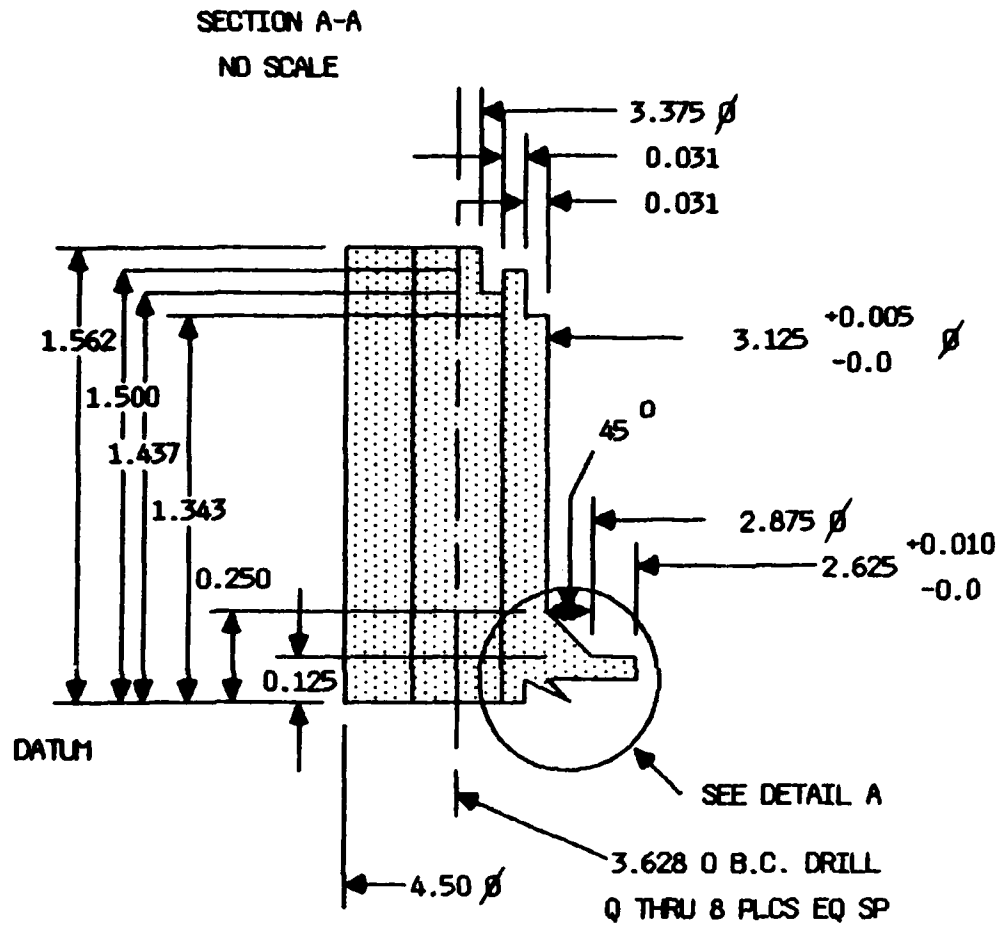

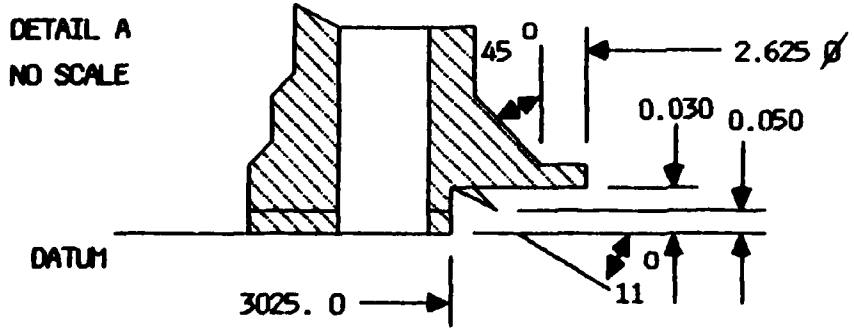

MATL: 304 ST STL
QTY: 1

FIGURE 1A

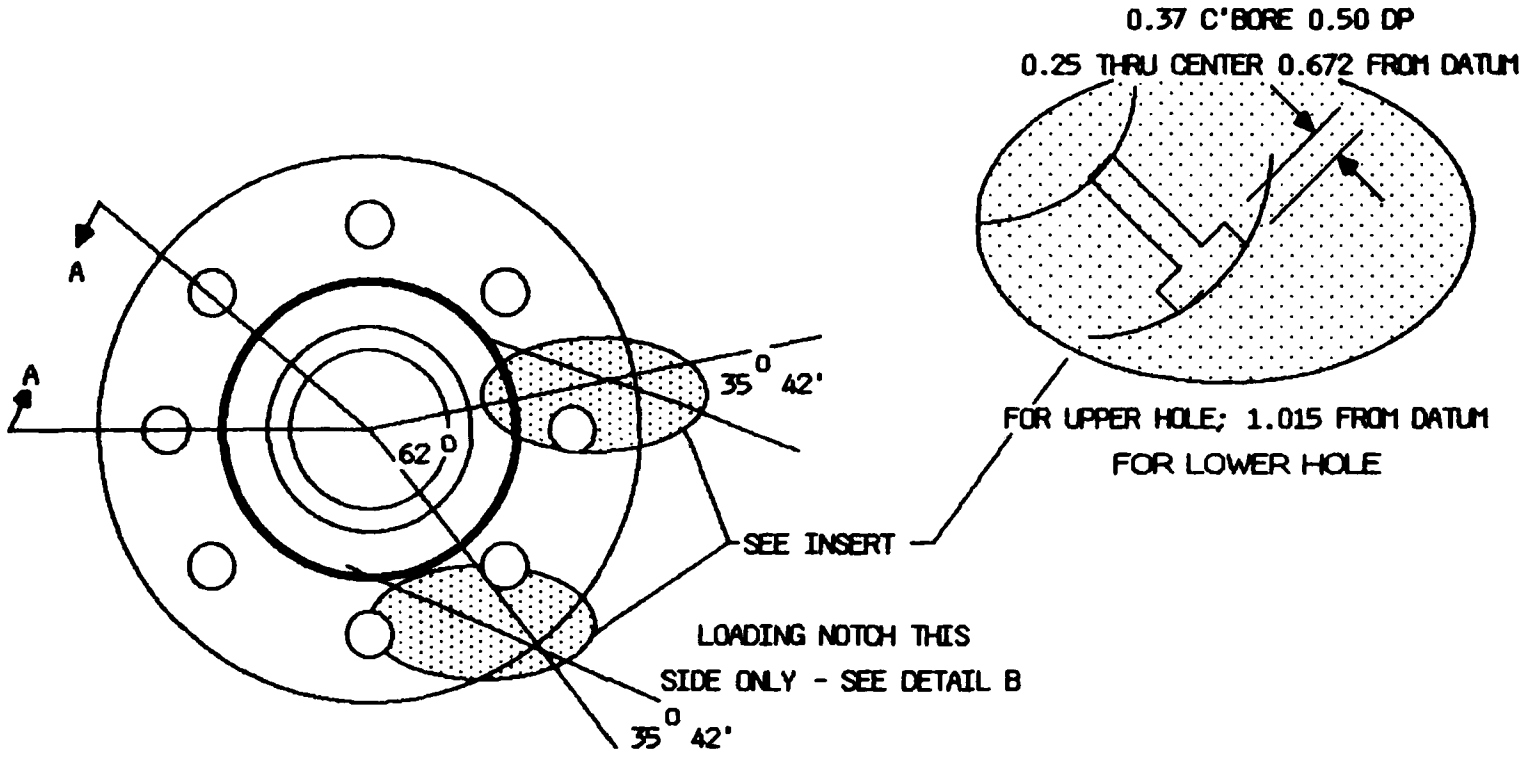
0.37 C'BORE 0.50 DP
0.25 THRU CENTER 0.672 FROM DATUM
A
A
35° 42'
62°
FOR UPPER HOLE; 1.015 FROM DATUM
FOR LOWER HOLE
SEE INSERT
LOADING NOTCH THIS
SIDE ONLY - SEE DETAIL B
35° 42'

FIGURE 1B

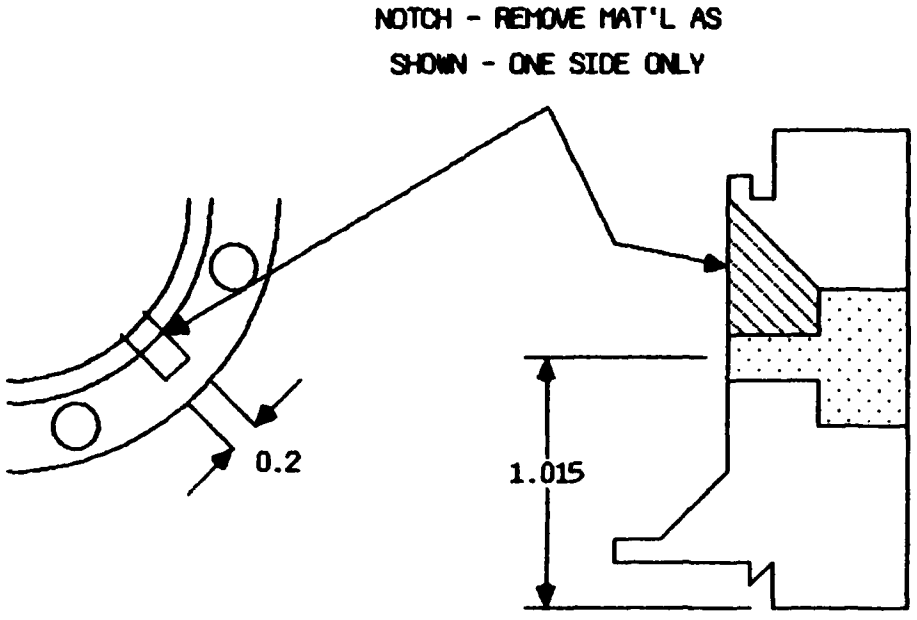

DETAIL B
NO SCALE

FIGURE 1C

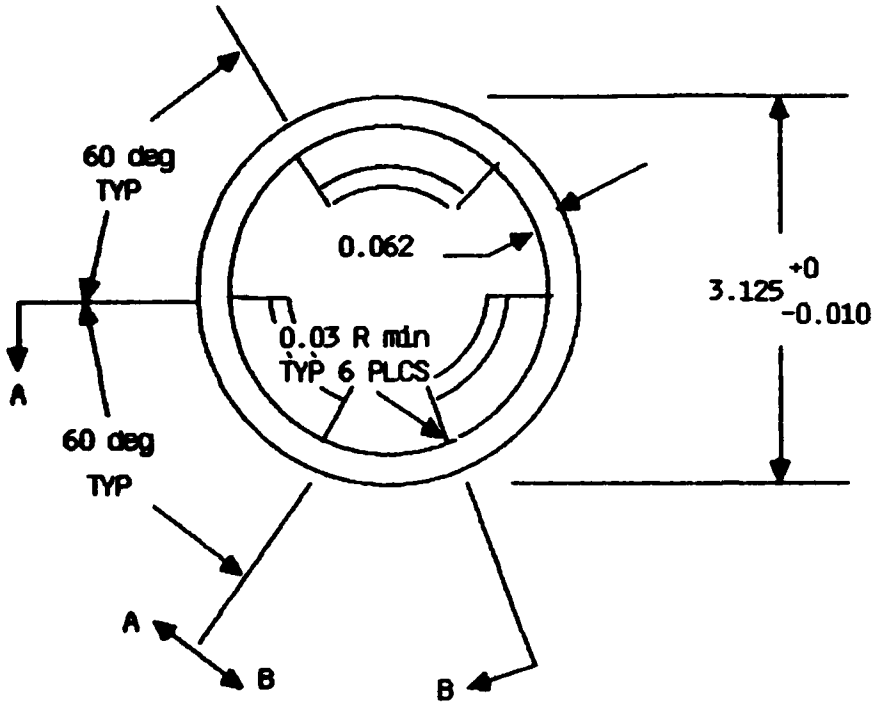

SECTION B-B NO SCALE

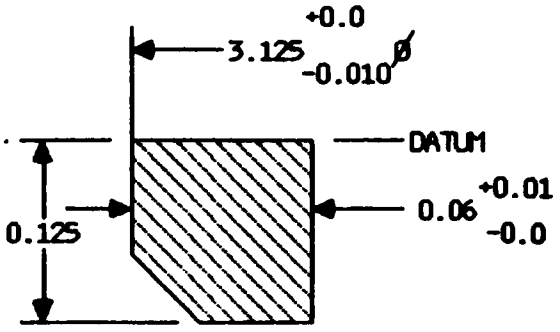

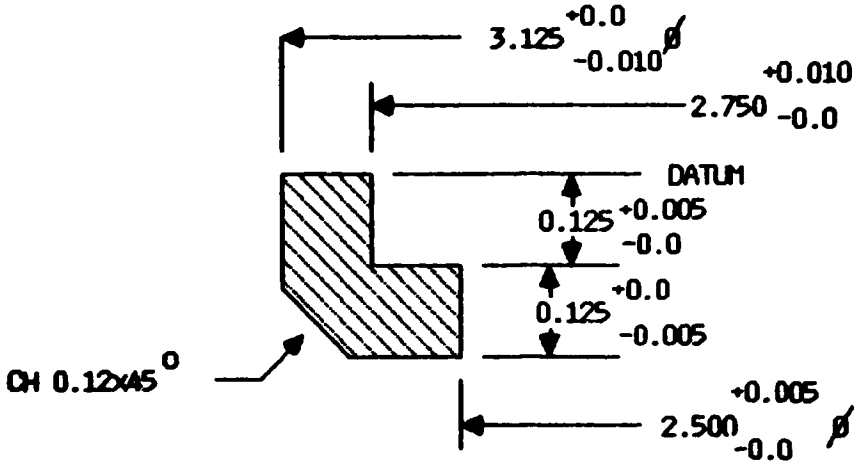

SECTION A-A NO SCALE

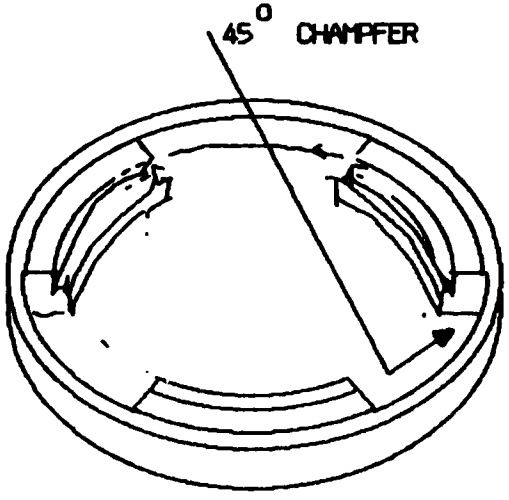

ISOMETRIC VIEW

MATL: VESPEL QTY: 1

FIGURE 2

SECTION A-A

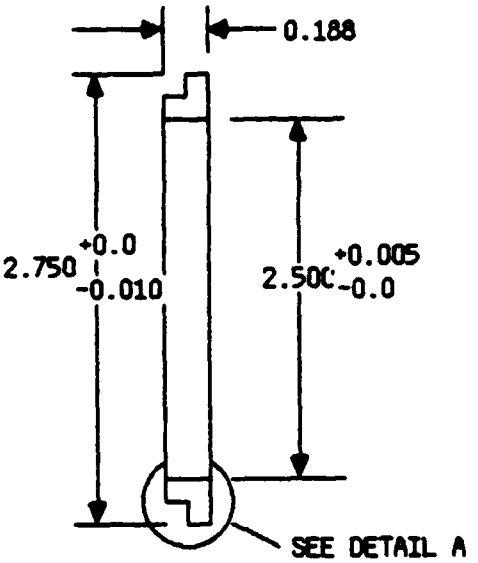

DETAIL A - NO SCALE

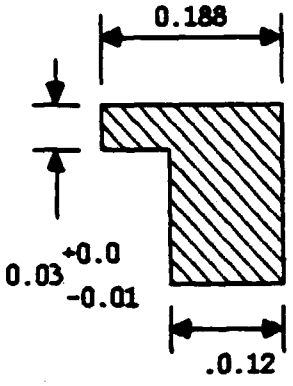

MATL: 304 ST STL

QTY: 1

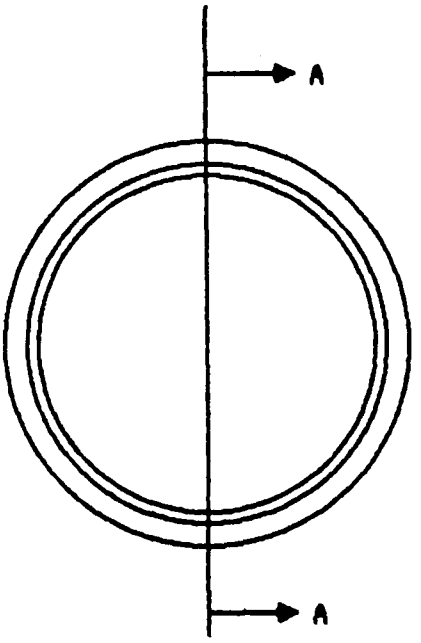

FIGURE 3

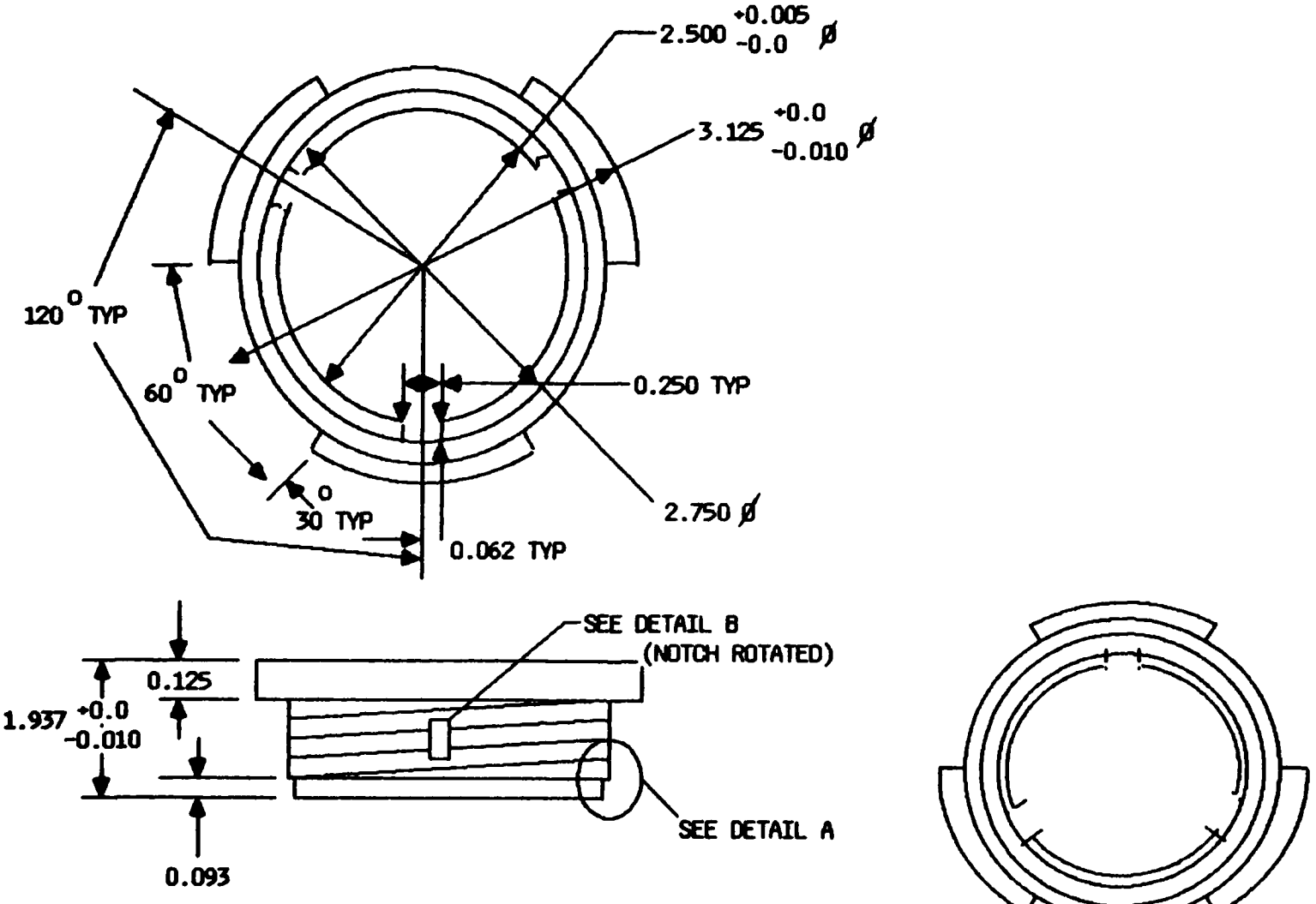
2.500 +0.005 -0.0 ø
3.125 +0.0 -0.010 ø
120° TYP
60° TYP
0.250 TYP
2.750 ø
30° TYP
0.062 TYP
SEE DETAIL B
(NOTCH ROTATED)
0.125
1.937 +0.0 -0.010
SEE DETAIL A
0.093

FIGURE 4A

DETAIL A - NO SCALE

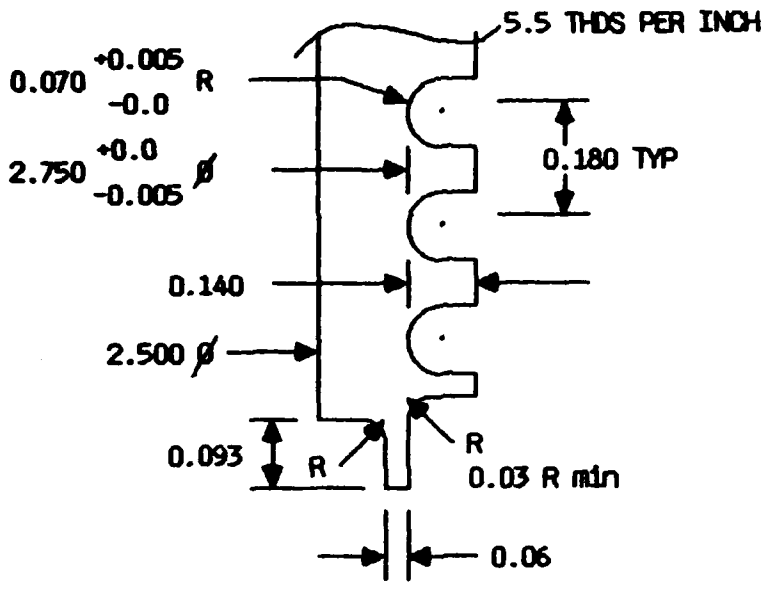

DETAIL B - NO SCALE

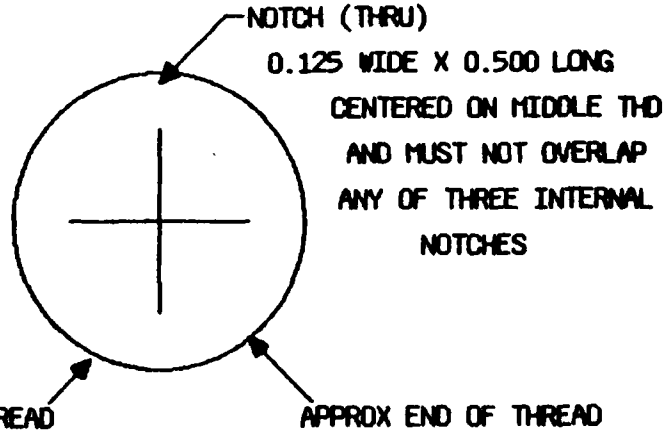

MATL: VESPEL

QTY: 1

FIGURE 4B

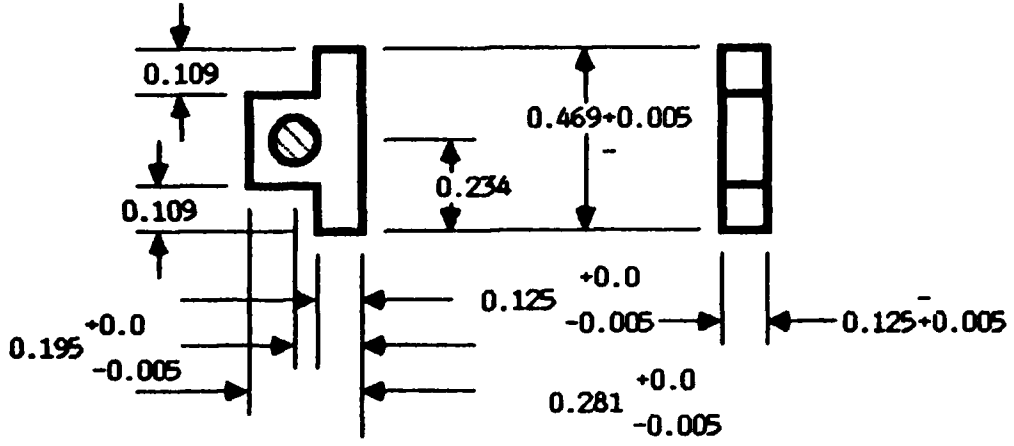

MATL: ST STL 304

QTY: 1

DRILL HOLE NO 30 DRILL

FIGURE 5

The upper part of the spool which supports the antenna against canting, is half cut away for pumping purposes. The gap between the outer edge of the spool threads and the interior of the flange is 0.10-0.11, which should keep the wire rope from jumping out of the thread while still allowing satisfactory pumping.

The tubes and flanges (Figures 6 and 7) connect holes A, B in the main flange (Figure 1) with the bellows that provide the flexible coupling to the outside world.

The waveguide itself is made in three main parts. The long tube (Figure 8) is attached to the step-plate reflector (Figure 9) and then to the extension (Figure 10). The tabs (Figure 11) are welded onto the waveguide near the top and lock with the notches in the VESPEL spool (Figure 4).

The "armor" shown in Figure 12 is a 0.125 inch wall tube with a hole cut out, through which the antenna radiates. The rods (Figure 13) are welded into holes A and B in the armor. The remaining pieces (Figures 14-16, and weldment Figure 17) make up the support for the armor and connect to the pivot on the tokamak floor. The holes in the upper piece (Figure 14), which is welded to the armor, pumps the space under the antenna extension. Figure 18 represents the assembled antenna showing the BeO window and the microwave mirror used to out couple the radiation.

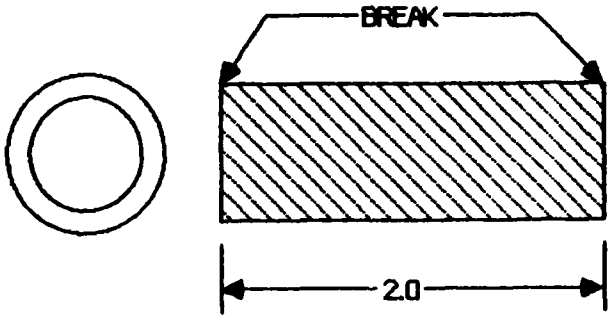

MTL: 304 ST STL TUBE, 0.37 O.D., 0.06 WALL

QTY: 2

FIGURE 6

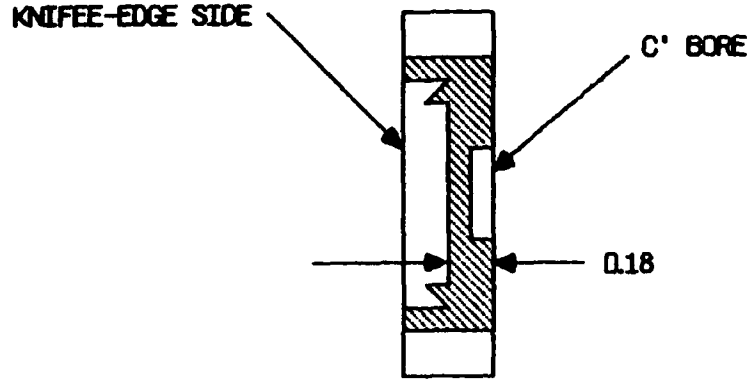

SECTION A-A

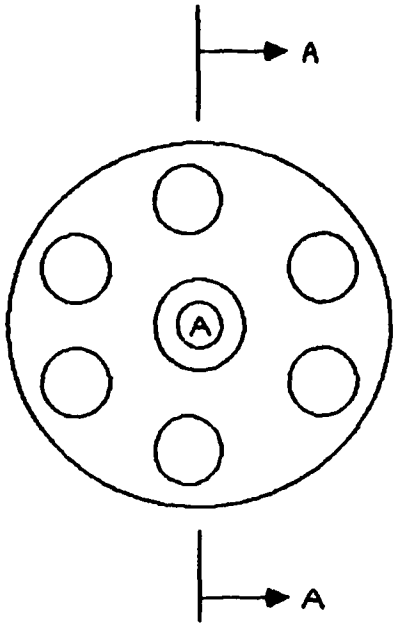

MATL: ST STL (SUPPLIED)
QTY: 2

HOLE DATA
A DRILL 0.25 THRU C' BORE
0.37 X 0.18 DP, 1 PLC

FIGURE 7

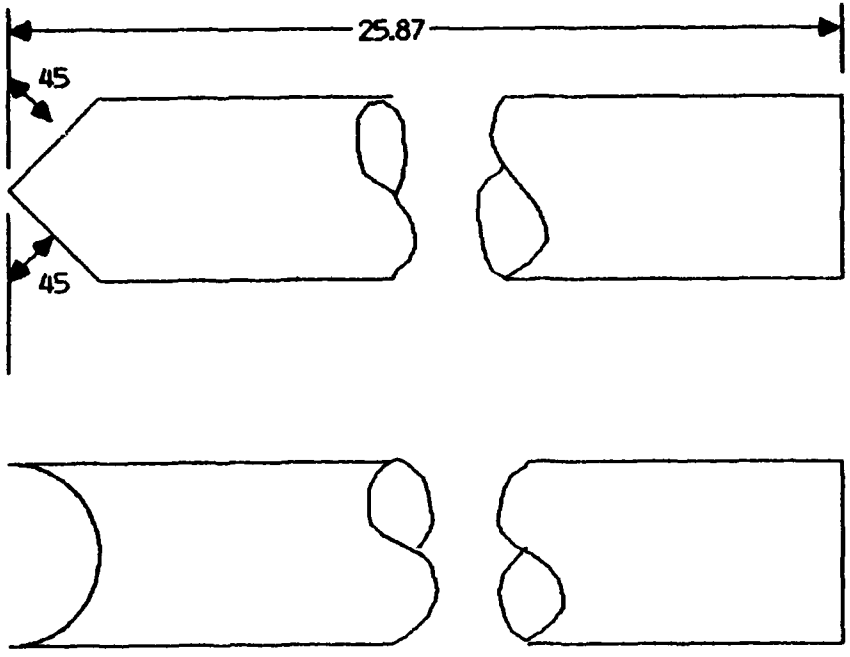

MATL: 304 ST STL TUBE, 0.06 WALL, 2.500 OD

QTY: 1

FIGURE 8

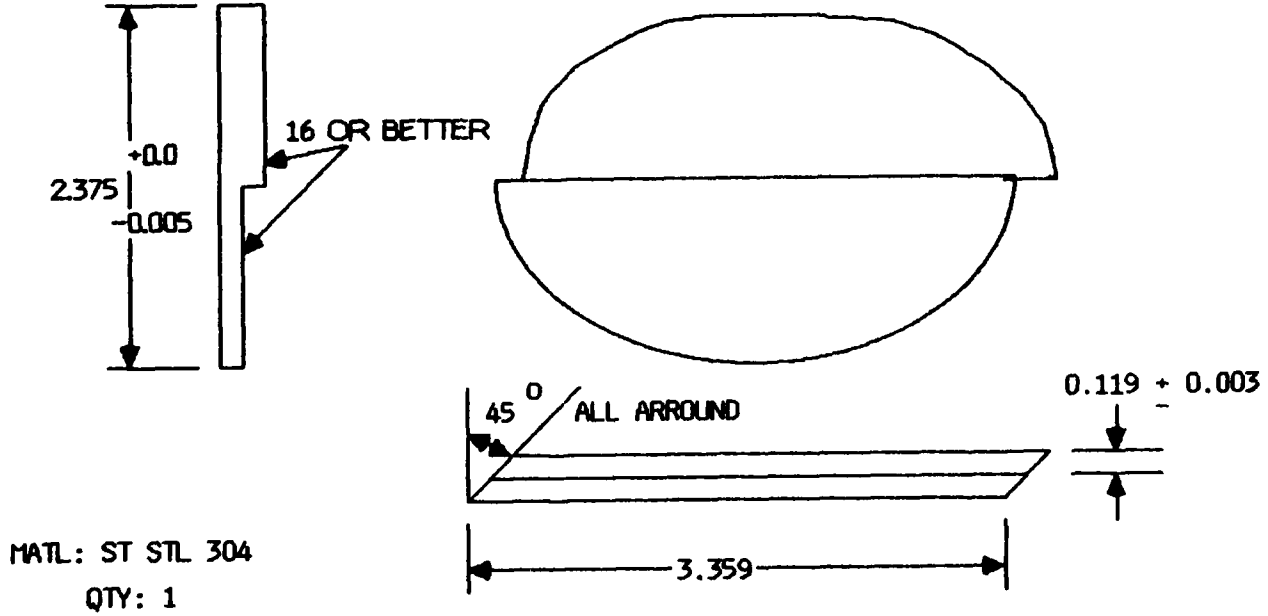

MATL: ST STL 304

QTY: 1

FIGURE 9

HOLE DATA

A & B - 0.12 THRU BOTH WALLS

NOTCHES ARE 90° APART

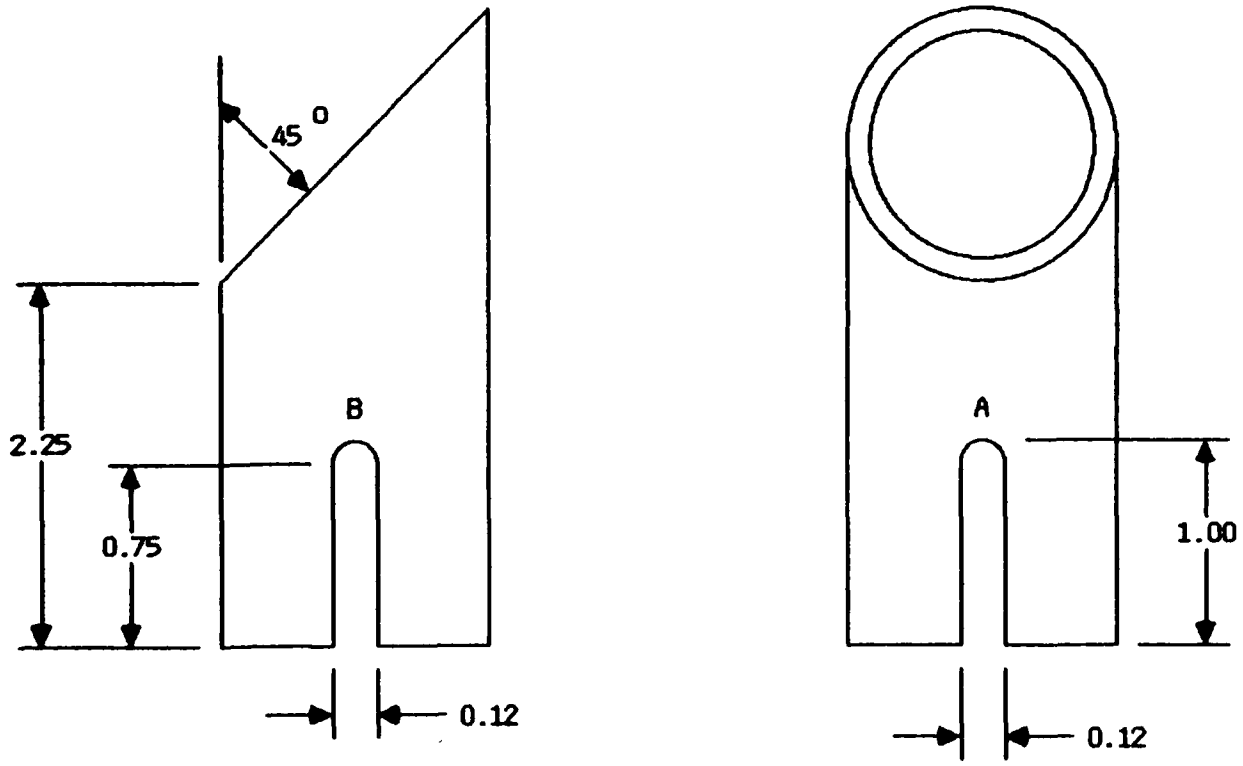

MATL: 304 ST STL TUBE, 0.06 WALL, 2.500 OD

QTY: 1

FIGURE 10

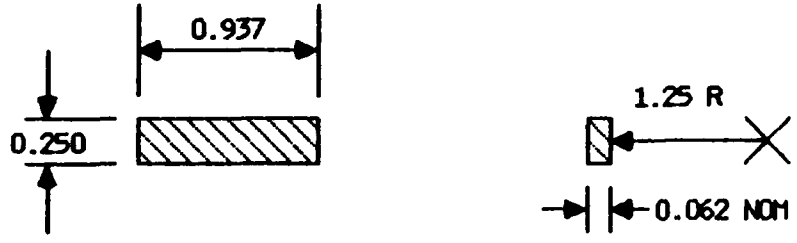

MATL: 304 ST STL

QTY: 3

FIGURE 11

HOLE DATA

A & B 0.12 THRU BOTH WALLS

HOLES 90° APART AS INDICATED

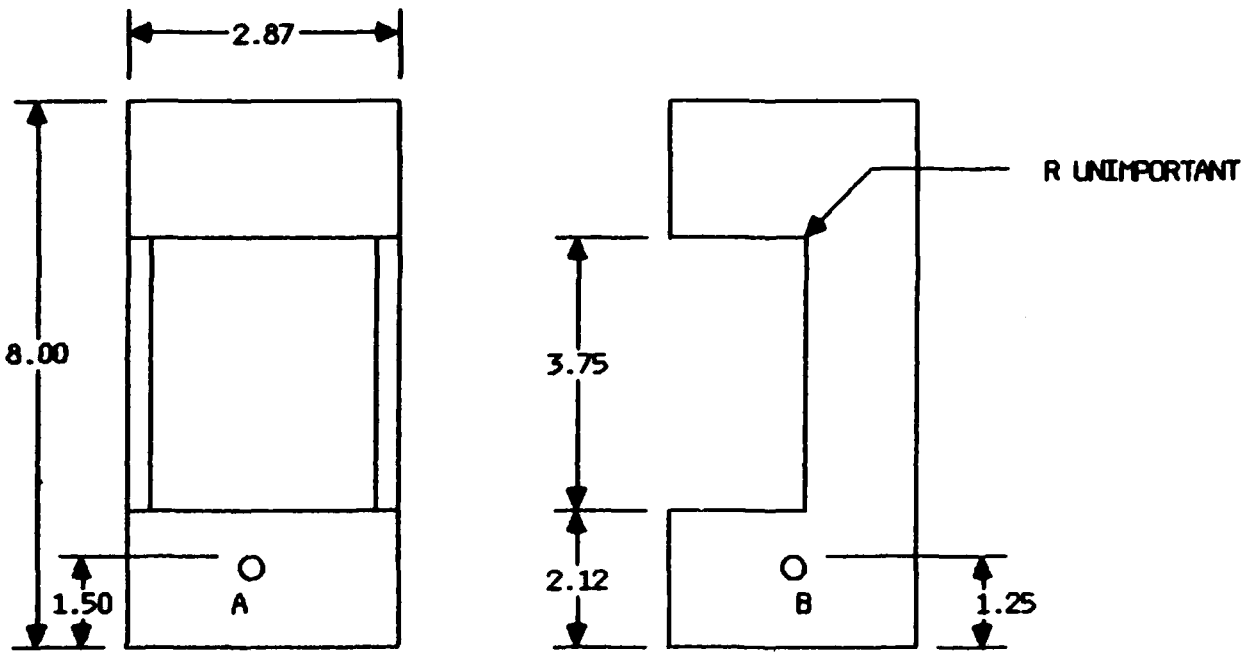

MATL: 304 ST STL TUBE, 0.125 WALL

QTY: 1

FIGURE 12

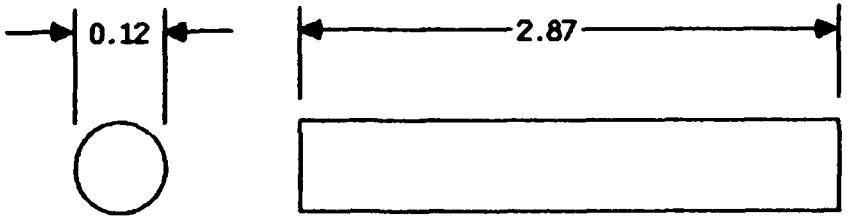

MATL: 304 ST STL, 0.125 NOM ROUND ROD
QTY: 2

FIGURE 13

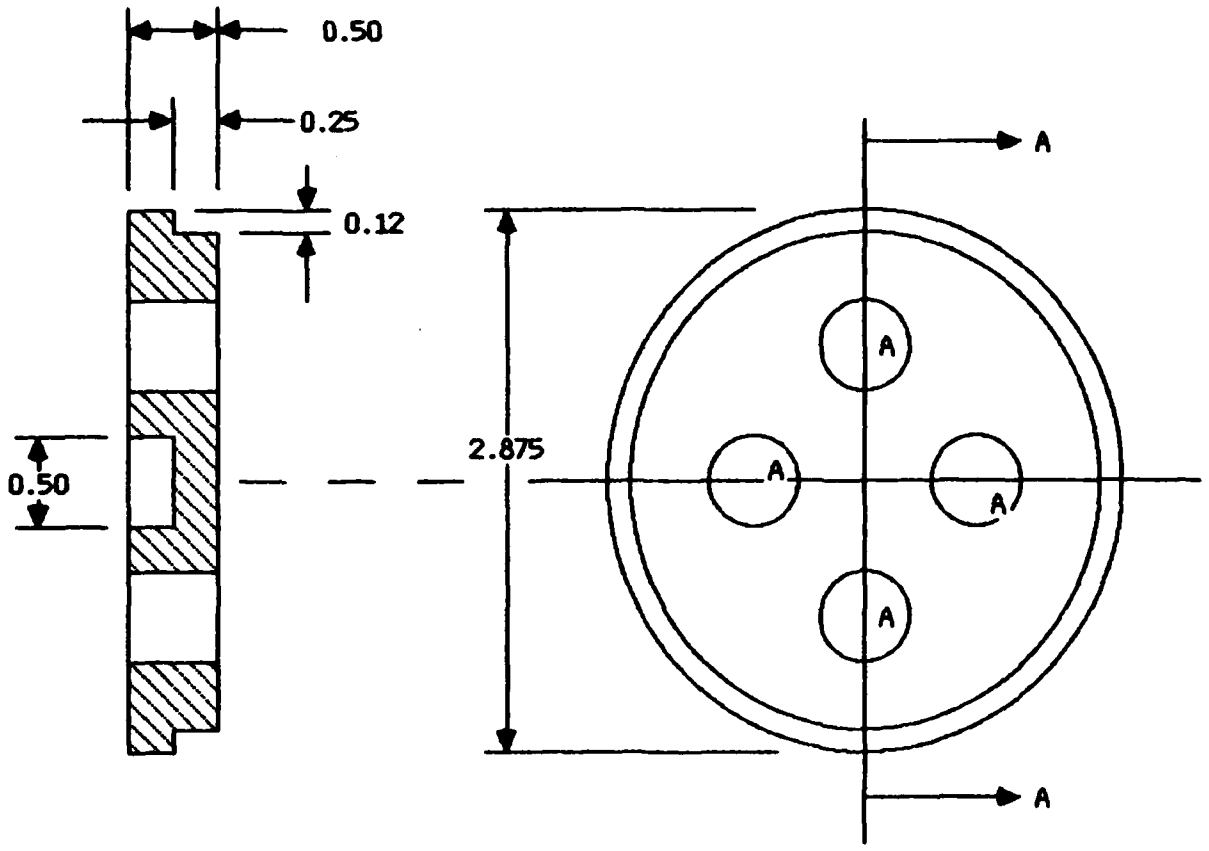

SECTION A-A

HOLE DATA
A - 0.5 THRU ON 1.5 BC
APPROX EQ SP, 4 PLCS
P/N - 002

MATL: 304 ST STL
QTY: 1

FIGURE 14

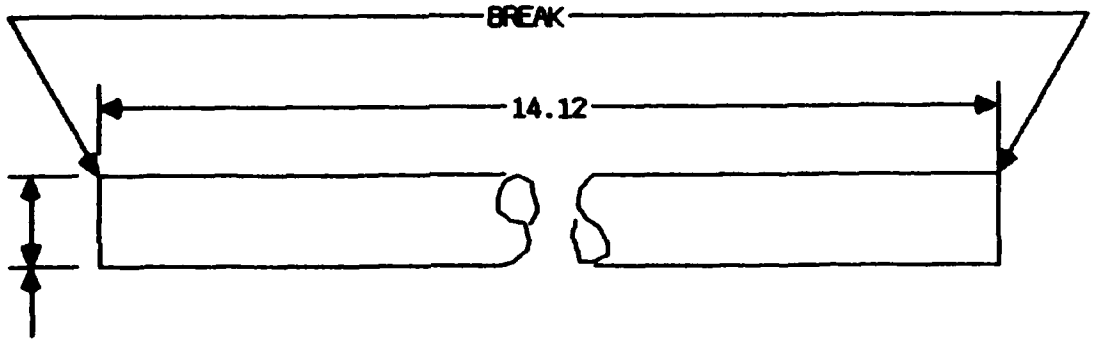

0.05 NOM
MUST FIT INTO 0.5 CTR HOLE
IN P/N -001, -002
SEE WELDMENT

MATL: 304 ST STL
QTY: 1

P/N -003

FIGURE 15

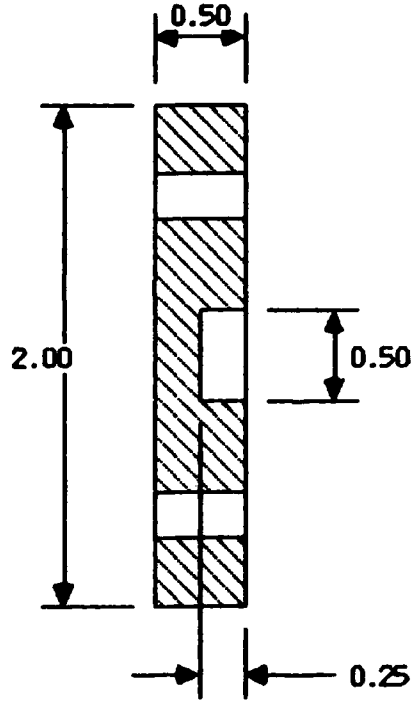

SECTION A-A

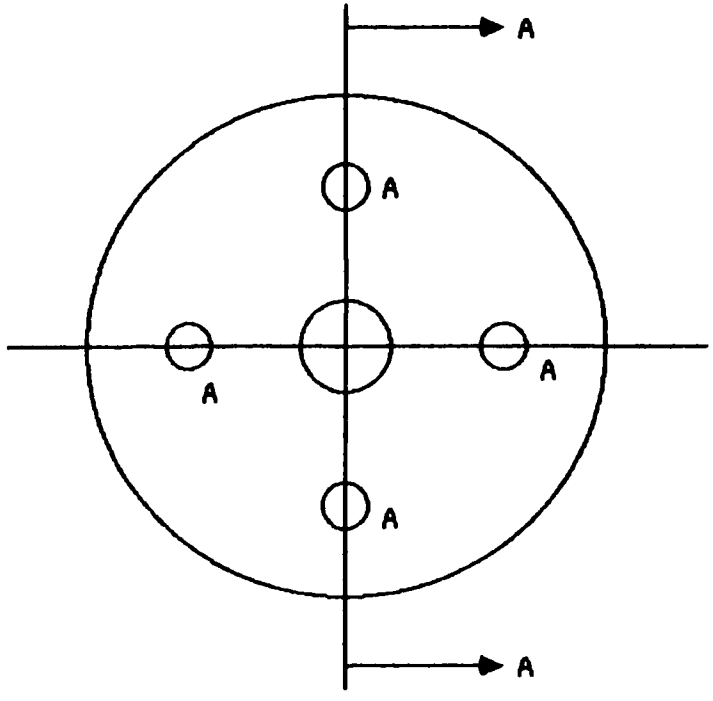

HOLE DATA
A - DRILL NO 27 THRU, 4 PLCS
EQ SP ON 1.375 B.C.

MATL: 304 ST STL
QTY: 1

P/N -001

FIGURE 16

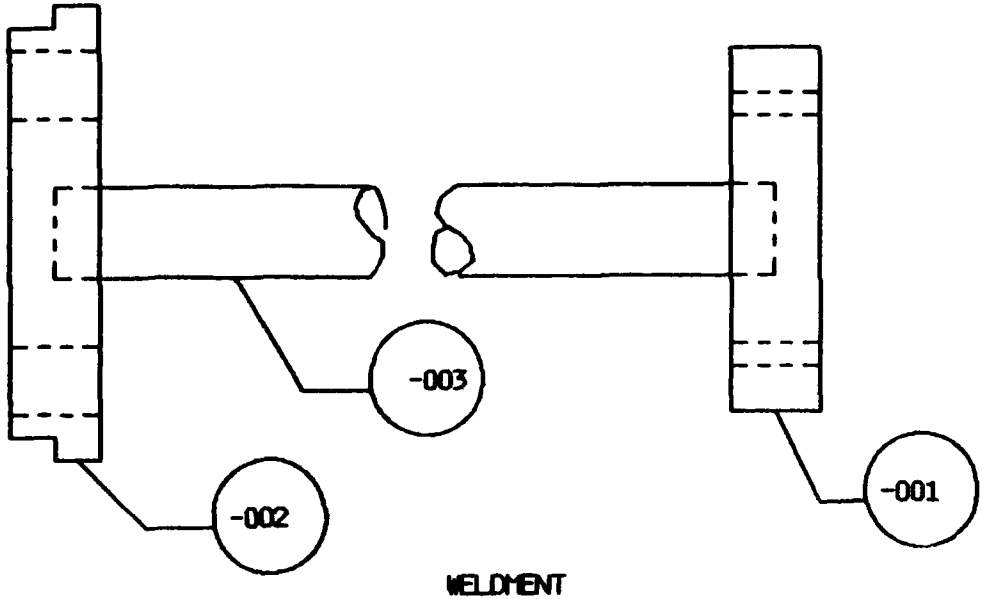

FIGURE 17

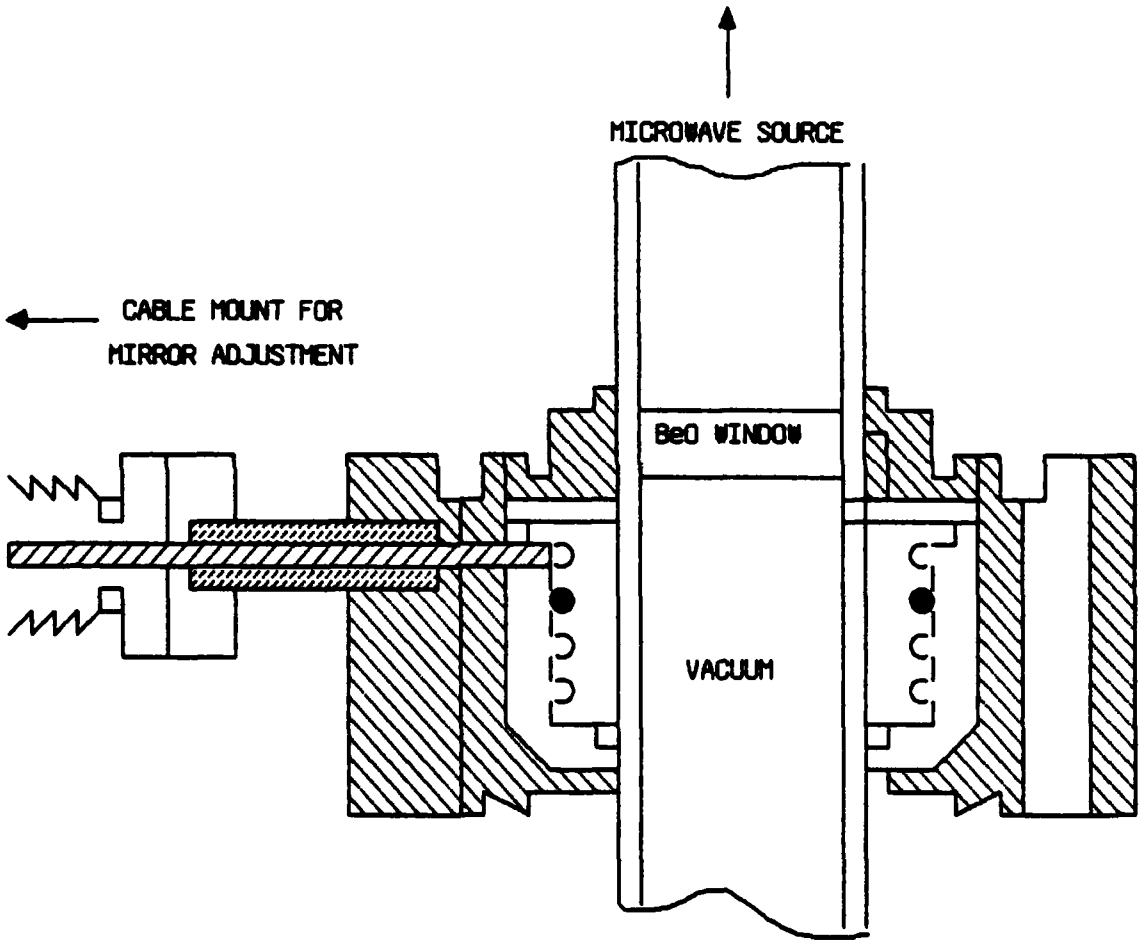
MICROWAVE SOURCE
CABLE MOUNT FOR
MIRROR ADJUSTMENT
BeO WINDOW
VACUUM

FIGURE 18A

FIGURE 18A

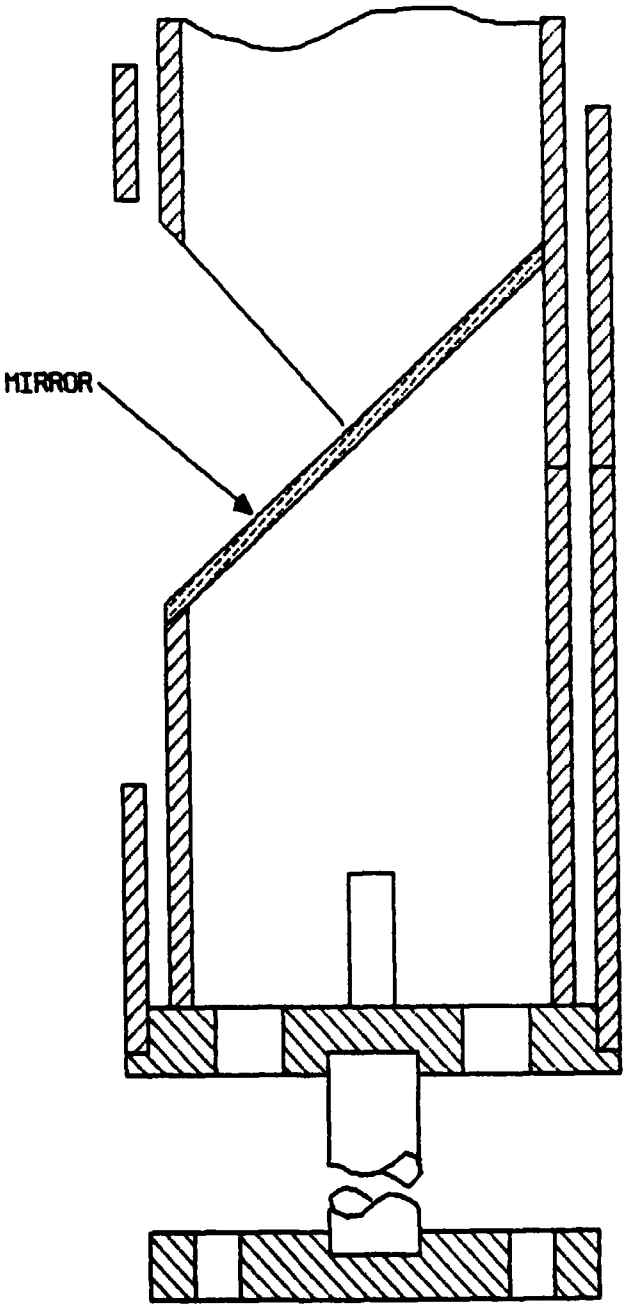

FIGURE 18B

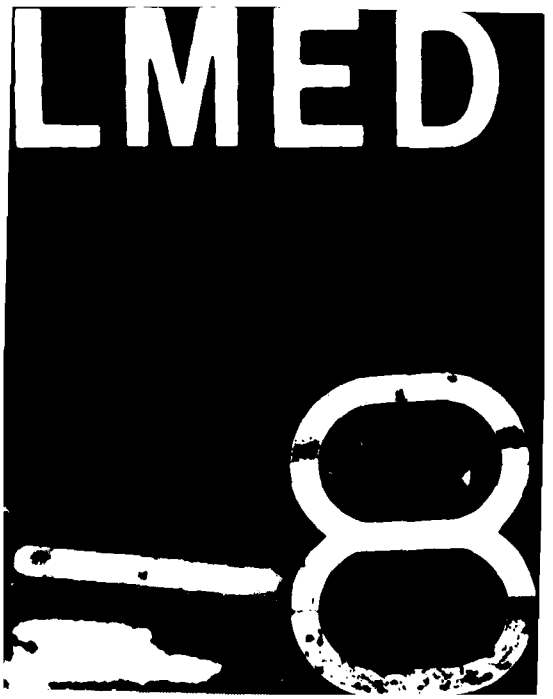
LMED